Indoxyl-sulfate activation of the AhR- NF-κB pathway promotes interleukin-6 secretion and the subsequent osteogenic differentiation of human valvular interstitial cells from the aortic valve

Alexandre Candellier, Nervana Issa, Maria Grissi, Théo Brouette, Carine Avondo, Cathy Gomila, Gérémy Blot, Brigitte Gubler, Gilles Touati, Youssef Bennis, et al.

Journal of Molecular and Cellular Cardiology 179 (2023) 18–29

Contents lists available at ScienceDirect

Journal of Molecular and Cellular Cardiology

journal homepage: www.elsevier.com/locate/yjmcc

Indoxyl-sulfate activation of the AhR- NF-κB pathway promotes interleukin-6 secretion and the subsequent osteogenic differentiation of human valvular interstitial cells from the aortic valve

Alexandre Candellier [a,b,1], Nervana Issa [a,1], Maria Grissi [a], Théo Brouette [a], Carine Avondo [a], Cathy Gomila [a], Gérémy Blot [a], Brigitte Gubler [c,d,e], Gilles Touati [f], Youssef Bennis [a], Thierry Caus [a,f], Michel Brazier [a,g], Gabriel Choukroun [a,b], Christophe Tribouilloy [a,h], Saïd Kamel [a,g], Cédric Boudot [a,2], Lucie Hénaut [a,*,2], On Behalf Of The Stop-As Investigators

[a] UR UPJV 7517, MP3CV, CURS, Université de Picardie Jules Verne, Amiens, France
[b] Department of Nephrology Dialysis and Transplantation, Amiens University Hospital, Amiens, France
[c] Department of Immunology, Amiens University Hospital, Amiens, France
[d] Department of Molecular Oncobiology, Amiens University Hospital, 80054, France
[e] EA4666 – HEMATIM, CURS, Picardie Jules Verne University, Amiens 80054, France
[f] Department of Cardiac Surgery, Amiens University Hospital, Amiens, France
[g] Department of Biochemistry, Amiens University Hospital, Amiens, France
[h] Department of Cardiology, Amiens University Hospital, Amiens, France

ARTICLE INFO

Keywords:
indoxyl sulfate
aortic stenosis
valvular interstitial cell
inflammation

ABSTRACT

Background: Calcific aortic stenosis (CAS) is more prevalent, occurs earlier, progresses faster and has worse outcomes in patients with chronic kidney disease (CKD). The uremic toxin indoxyl sulfate (IS) is powerful predictor of cardiovascular mortality in these patients and a strong promoter of ectopic calcification whose role in CAS remains poorly studied. The objective of this study was to evaluate whether IS influences the mineralization of primary human valvular interstitial cells (hVICs) from the aortic valve.

Methods: Primary hVICs were exposed to increasing concentrations of IS in osteogenic medium (OM). The hVICs' osteogenic transition was monitored by qRT-PCRs for *BMP2* and *RUNX2* mRNA. Cell mineralization was assayed using the o-cresolphthalein complexone method. Inflammation was assessed by monitoring NF-κB activation using Western blots as well as IL-1β, IL-6 and TNF-α secretion by ELISAs. Small interfering RNA (siRNA) approaches enabled us to determine which signaling pathways were involved.

Results: Indoxyl-sulfate increased OM-induced hVICs osteogenic transition and calcification in a concentration-dependent manner. This effect was blocked by silencing the receptor for IS (the aryl hydrocarbon receptor, AhR). Exposure to IS promoted p65 phosphorylation, the blockade of which inhibited IS-induced mineralization. Exposure to IS promoted IL-6 secretion by hVICs, a phenomenon blocked by silencing AhR or p65. Incubation with an anti-IL-6 antibody neutralized IS's pro-calcific effects.

Conclusion: IS promotes hVIC mineralization through AhR-dependent activation of the NF-κB pathway and the subsequent release of IL-6. Further research should seek to determine whether targeting inflammatory pathways can reduce the onset and progression of CKD-related CAS.

1. Introduction

Calcific aortic stenosis (CAS) is highly prevalent in patients with chronic kidney disease (CKD) and kidney failure [1]. The pathophysiological remodeling of the valve leaflets occurs about 10 years earlier, progresses faster and is associated with worse outcomes in people with

* Corresponding author at: UR UPJV 7517, MP3CV, CURS, Université de Picardie Jules Verne, Avenue René Laennec, F-80054 Amiens, France
E-mail address: lucie.henaut@u-picardie.fr (L. Hénaut).
[1] These authors contributed equally to the work and are joint first authors.
[2] These authors contributed equally to the work and are joint last author.

https://doi.org/10.1016/j.yjmcc.2023.03.011
Received 4 January 2023; Received in revised form 24 February 2023; Accepted 23 March 2023
Available online 24 March 2023

CKD, relative to people with normal renal function [2,3]. To date, drug therapies have been ineffective in preventing the progression of CAS, and so surgical aortic valve replacement (AVR) remains the mainstay of management for patients with symptomatic CAS [4]. However, the mortality rate after AVR increases as the estimated glomerular filtration rate falls [5]. The treatment of CAS in patients on dialysis is especially challenging, given their higher comorbidity burden. Despite the use of less invasive alternatives (such as transcatheter AVR), the in-hospital mortality rate after AVR in patients on dialysis is twice that observed in patients without kidney disease [6]. In this context, a better understanding of the cellular and molecular mechanisms underlying aortic valve calcification in patients with CKD is likely to help physicians to improve clinical outcomes.

Aortic valvular interstitial cells (VICs) are the most abundant cell type in the aortic valve and have a crucial role in CAS and progressive obstruction of the valve. The degree of VIC calcification is a marker of CAS progression and a powerful predictor of adverse events [7]. A key step in the development of CAS is the transition of VICs to an osteoblast-like phenotype characterized by enhanced expression of osteogenic markers, such as runt-related transcription factor 2 (RUNX2), and bone morphogenetic protein 2 (BMP2) [8]. Their osteogenic activity is thought to be responsible for the mineralization associated with CAS [9]. It has been shown that several disease-specific risk factors (such as imbalanced mineral metabolism, inflammation, and hemodynamic disturbances) induce the rapid progression of CAS in patients with kidney failure [10]. However, the impact of uremic toxins on the phenotypic transition and calcification of human VICs (hVICs) has not yet been established.

The uremic toxin indoxyl sulfate (IS) is produced by the metabolism of dietary tryptophan in the gut. The accumulation of IS in the serum of patients with CKD is a known, independent risk factor for cardiovascular morbidity and mortality [11]. The positive correlation between serum IS levels and vascular calcification [11] suggests that IS has pro-calcific effects. Indeed, IS has repeatedly been shown to increase high-phosphate-induced osteogenic transition and subsequent calcification in aortic vascular smooth muscle cells in vitro [12,13]. In non-CKD hypertensive rats, the administration of IS promotes vascular calcification and the expression of osteogenic-specific markers [14]. The cytosolic ligand-dependent transcription factor aryl hydrocarbon receptor (AhR) mediates most of the harmful cardiovascular effects of IS [15–17]. The presence of AhR in aortic valve leaflets and the putative impact of IS on the calcification of the aortic valve have not previously been investigated.

The objectives of the present study were therefore to (i) determine whether exposure to IS influences the osteoblast-like transition and calcification of human VICs, and (ii) identify the cellular and molecular mechanisms involved in these processes.

2. Methods

2.1. Culture of hVICs

Human aortic tricuspid valves were collected from patients with CAS after valve replacement surgery at Amiens Picardie University Hospital (Amiens, France). In accordance with French legislation, the patients gave their informed consent to the valves' use for research purposes. The study was approved by the local institutional ethics committee (approval reference: PI2021_843_0002). The hVICs were isolated from non-calcified areas of the valves and characterized as described previously [18,19]. Briefly, non-calcified valve fragments were incubated for 10 min at 37°C in Hanks' Balanced Salt Solution (#H6648, Sigma Aldrich) supplemented with 0.15% collagenase type A (#10103586001, Sigma Aldrich) and vortexed every 2 minutes to remove the monolayer of valvular endothelial cells (VEC). Fragments were then washed with saline, cut into 2 mm^2 explants and incubated overnight at 37°C under gentle agitation in DMEM medium (#D6546, Sigma Aldrich) containing 0.15% collagenase type A. The resulting cell suspension was then sieved (pore size: 70 μm) and centrifuged for 5 min at 1200 rpm. The harvested cells were then seeded (800 000 cells per 75 cm^2 flask) and cultured in complete DMEM containing 10% fetal bovine serum. This step marks the first passage. Only primary hVICs cultures staining negative for VECs markers (Von Willebrand factor and PECAM-1) were used in the experiments. Experiments were performed on cells from passages 2 to 6.

2.2. Indoxyl sulfate preparation

The concentrations of IS (#I3875, Sigma-Aldrich) used in our experiments were chosen according to the EUToX uremic solutes database (http://eutoxdb.odeesoft.com/index.php.), which provides an encyclopedic list of uremic toxins containing their mean normal plasmatic concentration, their highest mean/median uremic plasmatic concentration and their highest plasmatic concentration ever reported in uremia. Therefore, in our study hVICS were exposed to three concentrations of IS: IS normal (ISn): 0.5 μg/mL = 2 μmol/l; IS uremic (ISu): 37 μg/mL = 148 μmol/l; and IS maximum (ISmax): 233 μg/mL = 934 μmol/l. Since IS is a potassium salt, a culture medium containing 233 μg/mL KCl (a concentration equivalent to the potassium present in the ISmax condition) was used as a negative control (CT). This CT condition is represented by a dotted line in every graph presented in the manuscript.

2.3. The hVIC mineralization assay

To study the impact of IS on cell mineralization, hVICs (7500 cells per well, in 48-well plates) were exposed for 14 days to ISn, ISu or ISmax in the presence or absence of osteogenic medium (OM) containing 2.2 mmol/l calcium and 2.2 mmol/l phosphate. This OM mimics the elevation of the calcium x phosphate product observed in CKD patients, which is one of the strongest inducer of cardiovascular calcification in this population. Medium containing 1.8 mmol/l calcium and 1.1 mmol/l phosphate was used as a non-calcific medium. The culture medium was renewed every 3 days during the calcification process. For mineralization experiments with transfected hVICs, the latter were re-transfected every 3 days to ensure optimal siRNA activity. To determine whether IL-6 secretion mediates IS pro-calcific effects, an antibody against IL-6 (10 μg/mL, #mab-hIL6, InvivoGen, San Diego, CA) was added to the culture medium for the 14 days of the mineralization experiment.

2.4. Detection of mineral deposition

Mineral deposition was assayed using the o-cresolphthalein complexone method or the alizarin red staining, as described in the Supplementary Methods.

2.5. Transfection with siRNAs

Human VICs were transfected with siRNA diluted in OptiMEM (Gibco, Carlsbad, CA), using Lipofectamine 2000 (#11668027, InvitroGen, Paisley, UK). SiRNAs targeting AhR (siAhR) and p65 (Silencer select Pre-designed siRNA #AM16706, ID:106524 and ID:109424, respectively; Ambion, Foster City, CA) were used at a concentration of 15 nM. Scrambled siRNA (Silencer Select Negative Control #1 siRNA, #AM4635, Ambion) served as a negative control.

2.6. RNA extraction and real-time PCR

Since mRNA extraction is not achievable on calcified cells, hVICs mRNA expression has been assessed after 3 days of exposure to adequate treatment. Briefly, mRNA was extracted from hVICs (80,000 cells per well, in 6-well plates) using an RNeasy® Mini Kit (Qiagen), according to the manufacturer's instructions. RNA was reverse-transcribed into cDNA using the High Capacity cDNA Reverse Transcription Kit (Applied Biosystems, Foster City, CA, USA), according to the manufacturer's

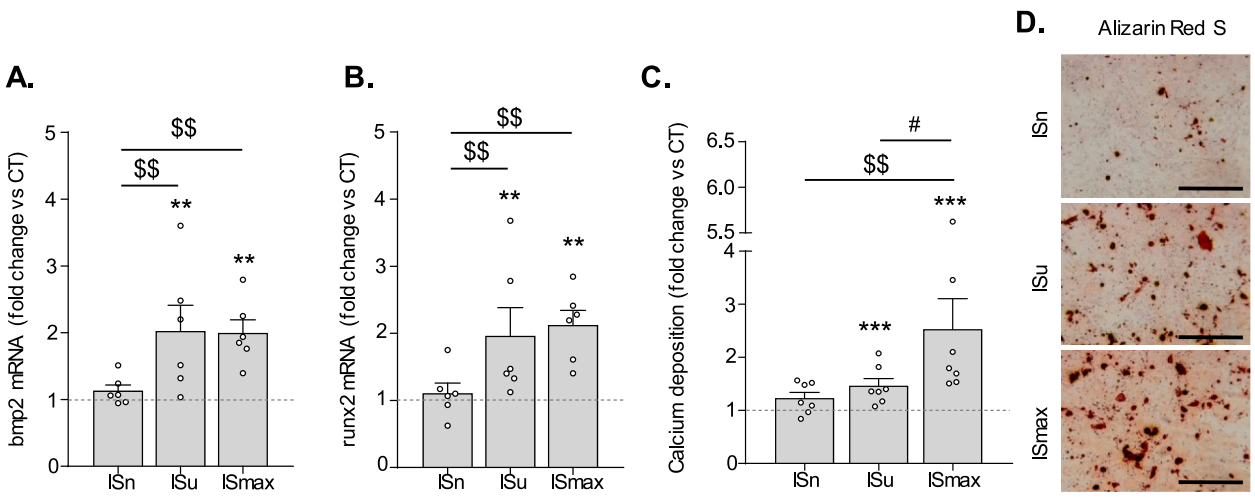

Fig. 1. Indoxyl-sulfate promotes OM-induced hVICs osteogenic transition and subsequent mineralization. To evaluate the impact of IS on OM-induced osteogenic transition and mineralization, hVICs were exposed for 3 or 14 days to either ISn, ISu or ISmax in presence of the OM. A. and B. Impact of a 3-day treatment with IS on bmp2 (A.) and runx2 (B.) mRNA expression, assessed by qRT-PCR. Results represent six independent experiments. Data are expressed as a fold change vs the control condition (CT: dotted line), which represents hVICs cultured in the absence of IS. Error bars represent the S.E.M. C. and D. Impact of a 14-day exposure to IS on the mineralization of hVICs cultured in the OM. A quantitative determination of calcium concentrations was performed by the O-cresolphtalein complexone method (C.). An alizarin red staining was performed to confirm the data (D.). Results represent seven independent experiments. For the quantification of mineral deposition, the mean calcium content per well (measured by the o-cresolphthalein complexone method) was normalized to the mean total protein content. Data are expressed as a fold-change relative to the control condition (CT: dotted line), which represents cells cultured in the absence of IS. Scale bars: 500µm. Error bars represent the S.E.M. $^{**}p<0.01$ and $^{***}p<0.001$ vs hVICs exposed to CT. $\$p<0.01$ vs hVICs exposed to ISn. $\#p<0.05$ vs hVICs exposed to ISu.

instructions. Real-time PCRs were performed on a StepOnePlus real-time PCR system (Applied Biosystems), using 2x SYBR® Green qPCR Master Mix (Applied Biosystems). The parameters for quantitative PCR are given in the Supplementary Methods. The sequences of the PCR primers for each gene are given in Supplementary Table 1. Levels of mRNA were normalized against that of the endogenous control (GAPDH), and the fold-change was calculated relative to the CT experiment.

2.7. Western blotting

Since protein extraction is not achievable on calcified cells, hVICs protein expression has been assessed after 3 days of exposure to adequate treatment. Briefly, hVICs (80,000 cells per well, in 6-well plates) were washed with PBS and then homogenized in lysis buffer (25 mM Tris-HCl, 150 mM NaCl, 5 mM EDTA, and 1% NP40, pH 7.4) containing phosphatase and protease inhibitor cocktails. The samples were shaken for 30 min and centrifuged, and the supernatant was collected. Proteins were assayed using the DC™ Protein Assay Kit (Bio-Rad) and stored at -80°C for later analysis. To study p65 nuclear translocation, hVICs (80,000 cells per well, in 6-well plates) were starved for 4 hours in complete DMEM without serum before to be exposed or nor to ISmax for 30 minutes. Cells were then lysed with the kit NE-PER™ to extract the proteins from the nuclear and cytoplasmic fractions separately (#78835, ThermoFisher Scientific), according to manufacturer's instruction. Western blotting was performed as described in the Supplementary Methods.

2.8. Detection of tumor necrosis factor alpha (TNF-α), interleukin (IL)-6 and IL-1β in hVIC supernatants

To study the effects of IS on the hVICs' secretion of pro-inflammatory cytokines, hVICs (7500 cells per well, in 48-well plates) were exposed for 3 days to ISn, ISu or ISmax in the presence or absence of the OM. Cell culture supernatants were then harvested, centrifuged 10 min at 13000 rpm to remove particles and assayed by sandwich ELISA using microfluidics Simple Plex cartridge™ for human TNF-α 2nd generation (SPCKB-PS-002803), human IL-6 2nd generation (SPCKB-PS-003028) and human IL-1β (SPCKB-PS-000216) (ProteinSimple, San Jose, California, USA) on Ella Automated Immunoassay System™ (Bio-Techne, Minneapolis, Minnesota, USA) following manufacturer's instructions.

2.9. Statistical analysis

The results represented at least five independent experiments (i.e. using cells isolated from different donors) performed in triplicate and were expressed as the mean ± standard error of the mean (SEM). The fold-changes were calculated relative to the CT condition, which is represented by a dotted line in every graph presented in the manuscript. All statistical analyses were performed using GraphPad Prism software (version 6.01, GraphPad Software Inc., San Diego, CA). Differences between two groups were assessed using the non-parametric Mann–Whitney test. The threshold for statistical significance was set to $p<0.05$.

3. RESULTS

3.1. Indoxyl sulfate accentuates the OM-induced osteogenic transition and calcification of hVICs

To evaluate the effects of IS on hVIC osteogenic transition and mineralization, hVICs were exposed to ISn (2 µmol/l), ISu (148 µmol/l) or ISmax (934 µmol/l) in the presence of an OM.

As presented in Supplementary Fig. 1, a 3-day exposure to the OM promoted hVICs osteogenic transition, evidenced by the elevation of the expression of the main osteogenic markers BMP2 and RUNX2 both at the mRNA (Supplementary Fig. 1.A and B) and protein (Supplementary Fig. 1.C-E) level. Exposure to this OM promoted hVIC mineralization within 14 days (Supplementary Fig. 1.F-H).

Interestingly, a 3-day exposure to ISu or ISmax promoted a 2-fold increase in OM-induced mRNA expression of *BMP2* ($p<0.05$) (Fig. 1.A) and *RUNX2* ($p<0.05$) (Fig. 1.B), relative to cells cultured in the absence of IS (control (CT) condition, represented by a dotted line in the graphs). If this increased osteogenic transition was not sufficient to promote OM-induced calcification after only 3 days of incubation (Supplementary Fig. 2), a 14-day exposure to IS increased OM-induced

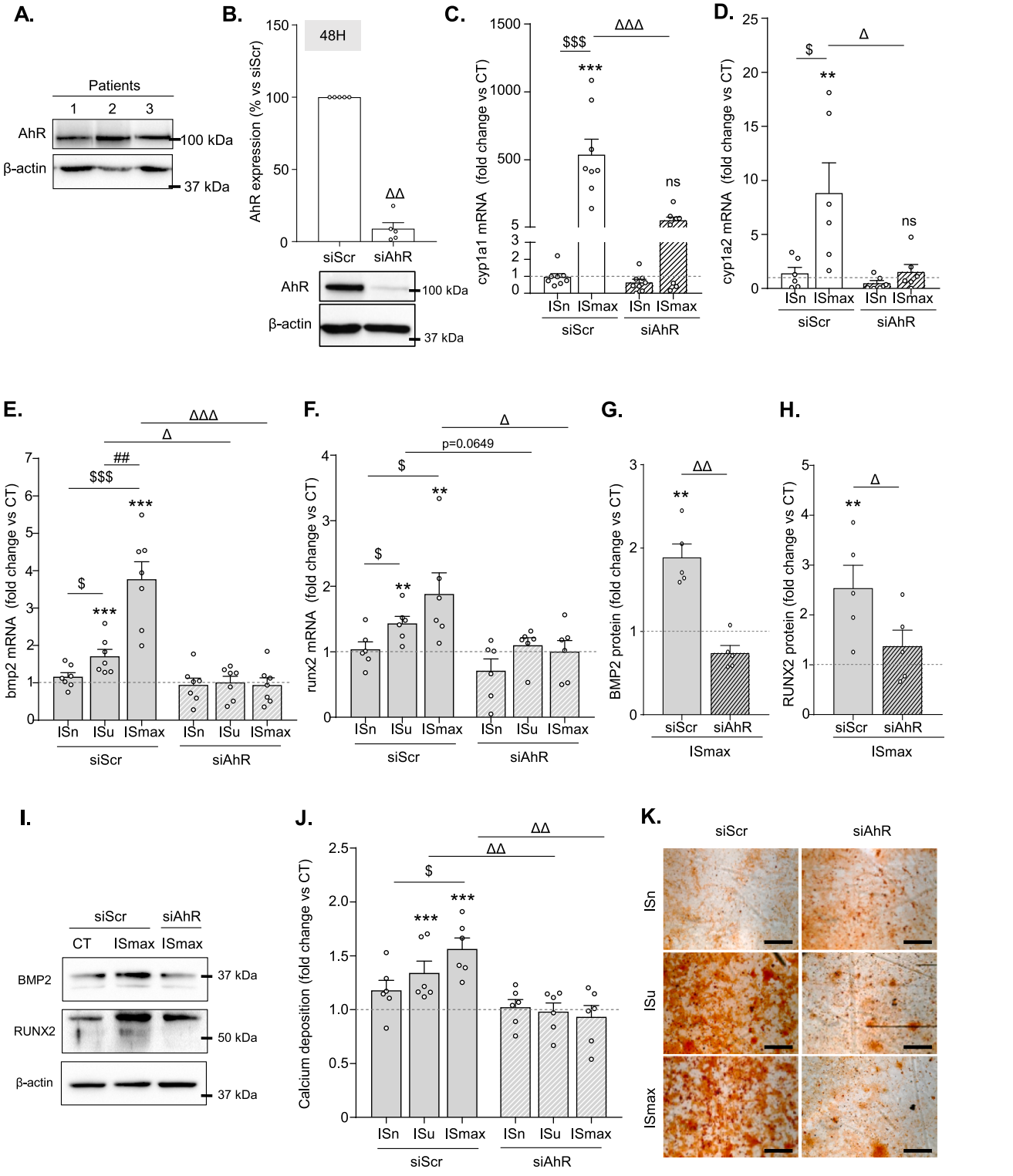

(caption on next page)

Fig. 2. Human VICs express a functional aryl hydrocarbon receptor (AhR), which plays a key role in IS-induced hVICs osteogenic transition and calcification. A. Western blot evaluation of AhR expression performed on whole cell lysates of human VICs isolated from 5 different donors. B. Effects of the siRNA targeting AhR on AhR expression in h-VICs. Results represent five independent experiments. Error bars represent the S.E.M. C—D. Expression of cyp1a1 (C.), cyp1a2 (D.) mRNA in hVICs transfected either with a siRNA targeting AhR or a scrambled siRNA and exposed for 3 days to ISn or ISmax in non-calcific condition. Results represent at least five independent experiments. Data are expressed as a fold change vs the control condition (CT: dotted line), which represents scramble-transfected cells cultured in the absence of IS. Error bars represent the S.E.M. E. and F. Impact of the siRNA targeting AhR on IS-induced expression of bmp2 (E.) and runx2 (F.) mRNA in hVICs cultured in the OM. Expression of bmp2 and runx2 transcripts was assessed by qRT-PCR following 3 days of treatment. Results represent at least six independent experiments. Data are expressed as a fold change vs the control condition (CT: dotted line), which represents scramble-transfected cells cultured in the absence of IS. Error bars represent the S.E.M. G.-I. Impact of a 3-day treatment with ISmax on BMP2 (G. and I.) and RUNX2 (H. and I.) protein expression in scrambled (siScr) or AhR-siRNA (siAhR) transfected hVICs exposed to the OM, assessed by western blot. Results represent five independent experiments. Data are expressed as a fold change vs the control condition (CT: dotted line), which represents scramble-transfected cells cultured in the absence of IS. Error bars represent the S.E.M. J. and K. Impact of the siRNA targeting AhR on IS-induced hVICs mineralization. The quantitative determination of calcium concentrations was performed by the O-cresolphtalein complexone method (J.). An alizarin red staining was performed to confirm the data (K.). Results represent six independent experiments. For the quantification of mineral deposition, the mean calcium content per well (measured by the o-cresolphthalein complexone method) was normalized to the mean total protein content. Data are expressed as a fold-change relative to the control condition (CT: dotted line), which represents scramble-transfected cells cultured in the absence of IS. Error bars represent the S.E.M. Scale bars: 500μm. Data are expressed as a fold change vs the control condition (CT: dotted line) which represents cells cultured in the absence of IS. Error bars represent the S.E.M. $^{**}p<0.01$ and $^{***}p<0.001$ vs hVICs exposed to CT. $\$p<0.05$ and $\$\$\$p<0.001$ vs hVICs exposed to ISn. ##p<0.01 vs hVICs exposed to ISu. Δp<0.05, ΔΔp<0.01 and ΔΔΔp<0.001 vs scrambled-transfected hVICs.

hVIC mineralization in a concentration-dependent manner, relative to CT cells (ISu: +46% vs. CT ($p<0.05$), ISmax: +153% vs. CT ($p<0.05$)) (Fig. 1.C and D). In contrast, treatment with ISn had no impact on OM-induced expression of *BMP2* or *RUNX2* or OM-driven mineralization, relative to CT cells (Fig. 1.A-D).

Interestingly, exposure to ISu and ISmax in the absence of the OM was also associated with significantly greater expression of *BMP2* and *RUNX2* by hVICs (Supplementary Fig. 3.A-E). However, in the absence of the OM this increased osteogenic transition was not sufficient to promote hVICs mineralization at day 14 (Supplementary Fig. 3.F and G). Interestingly, priming hVICs with IS for 7 days in the absence of the OM rendered them more prone to mineralize when subsequently washed out prior to be incubated solely with the OM (Supplementary Fig. 4.A and B). This demonstrates that the elevation of the calcium x phosphate product, which is a key feature in CKD patients, is mandatory to promote the mineralization of IS-induced osteoblast-like hVICs. Exposure to increasing concentrations of IS (whether under non-calcific or pro-calcific conditions) did not affect the hVICs' viability (Supplementary Fig. 5 and 6).

3.2. Human VICs express a functional AhR

Western blots performed on hVIC whole-cell lysates from five different patients showed that these cells express the IS receptor AhR (Fig. 2.A). To evaluate AhR's responsiveness to IS, hVICs transfected with either siAhR (which reduced AhR expression in hVICs by 80%; Fig. 2.B) or scrambled siRNA were exposed for 3 days to ISmax. The mRNA expression of two typical AhR-responsive genes (*CYP1A1* and *CYP1A2*) was monitored. In scrambled transfected cells, exposure to ISmax markedly enhanced the expression of both *CYP1A1* and *CYP1A2* mRNA (Fig. 2.C and D). In contrast, exposure to ISmax failed to promote the mRNA expression of *CYP1A1* and *CYP1A2* in hVICs transfected with siRNA targeting AhR (Fig. 2.C-D). These results showed that hVICs cultured in non-calcific conditions can indeed respond to IS via AhR.

3.3. Downregulation of AhR expression prevents the IS-induced osteogenic transition and calcification of hVICs

To determine whether the IS-induced osteogenic transition and calcification of hVICs depend on AhR activation, cells transfected with siAhR or scrambled-siRNA were exposed to ISn, ISu or ISmax in OM. Downregulation of AhR expression completely abolished the elevation of *BMP2* and *RUNX2* induced by IS both at the mRNA (Fig. 2.E and F) and protein level (Fig. 2.G-I). This effect was associated with a significant decrease in hVICs mineralization (Fig. 2.J and K). In our model, hVICs were transfected every 3 days in order to maintain a low level of AhR expression throughout the mineralization process. This treatment had no impact on cell viability (Supplementary Fig. 7).

3.4. IS-induced activation of the canonical NF-κB pathway promotes the osteogenic transition and calcification of hVICs

Inflammation induced through the NF-κB pathway is a potent driver of aortic valve calcification [20–22]. Since IS has been shown to promote NF-κB pathway in various cell types [16,23,24], we hypothesized that IS-induced hVIC mineralization is linked to NF-κB activation. To test this hypothesis, we first evaluated the impact of IS on IκBα degradation, p65 phosphorylation and p65 nuclear translocation, which are hallmarks of NF-κB pathway activation [25]. The results of the Western blot analysis showed that exposure to ISu and ISmax but not ISn was associated with significant, concentration-dependent decrease in IκBα expression (Fig. 3.A) and a significant, concentration-dependent increase in p65 phosphorylation (Fig. 3.B), relative to untreated cells. These effects were associated with the induction of p65 nuclear translocation (Fig. 3.C), which confirms the ability of IS to promote the activation of the NF-κB pathway in hVICs.

To further determine whether the NF-κB pathway is involved in the IS-induced osteogenic differentiation and mineralization of hVICs, we targeted p65 expression with siRNA approach. Transfection with the siRNA against p65 (which reduced p65 expression in hVICs by 80%; Fig. 3.D) blocked the accentuation of *BMP2* and *RUNX2* expression induced by IS under both pro-calcific conditions (Fig. 3.*E*-I) or non-calcific conditions (Supplementary Fig. 8.A and B). Transfection of hVICs with the siRNA against p65 also completely blocked the ability of ISu and ISmax to promote OM-induced hVIC mineralization, relative to transfection with the scrambled siRNA (Fig. 3.J and K). Transfection of hVICs with the siRNA against p65 did not modify cell viability, relative to cells treated with the scrambled siRNA (Supplementary Fig. 9).

3.5. IS promotes the hVICs' secretion of IL-6 and IL-1β but not TNF-α

Pro-inflammatory factors such as TNF-α, IL-1β and IL-6 drive myofibroblast-like hVICs to acquire an osteogenic phenotype and thereby promote the mineralization process [20,26]. Since the IS-induced NF-κB pathway promotes the secretion of these cytokines in various cell types [16,23,24,27], we hypothesized that IS's pro-calcific effects on hVICs depend on the secretion of these cytokines. To test this hypothesis, we first evaluated the ability of hVICs to secrete TNF-α, IL-1β and IL-6 under basal culture conditions. ELISAs showed that hVICs cultured under non-calcific conditions are unable to secrete detectable amounts of TNF-α but secrete very low amounts of IL-1β (mean ± SEM: 0.0915 ± 0.0421 pg/mL) and high levels of IL-6 (1037 ± 343.5 pg/mL) (Fig. 4.A). A 3-day exposure to the OM did not significantly modulate the hVICs' basal secretion of these cytokines (Fig. 4.A).

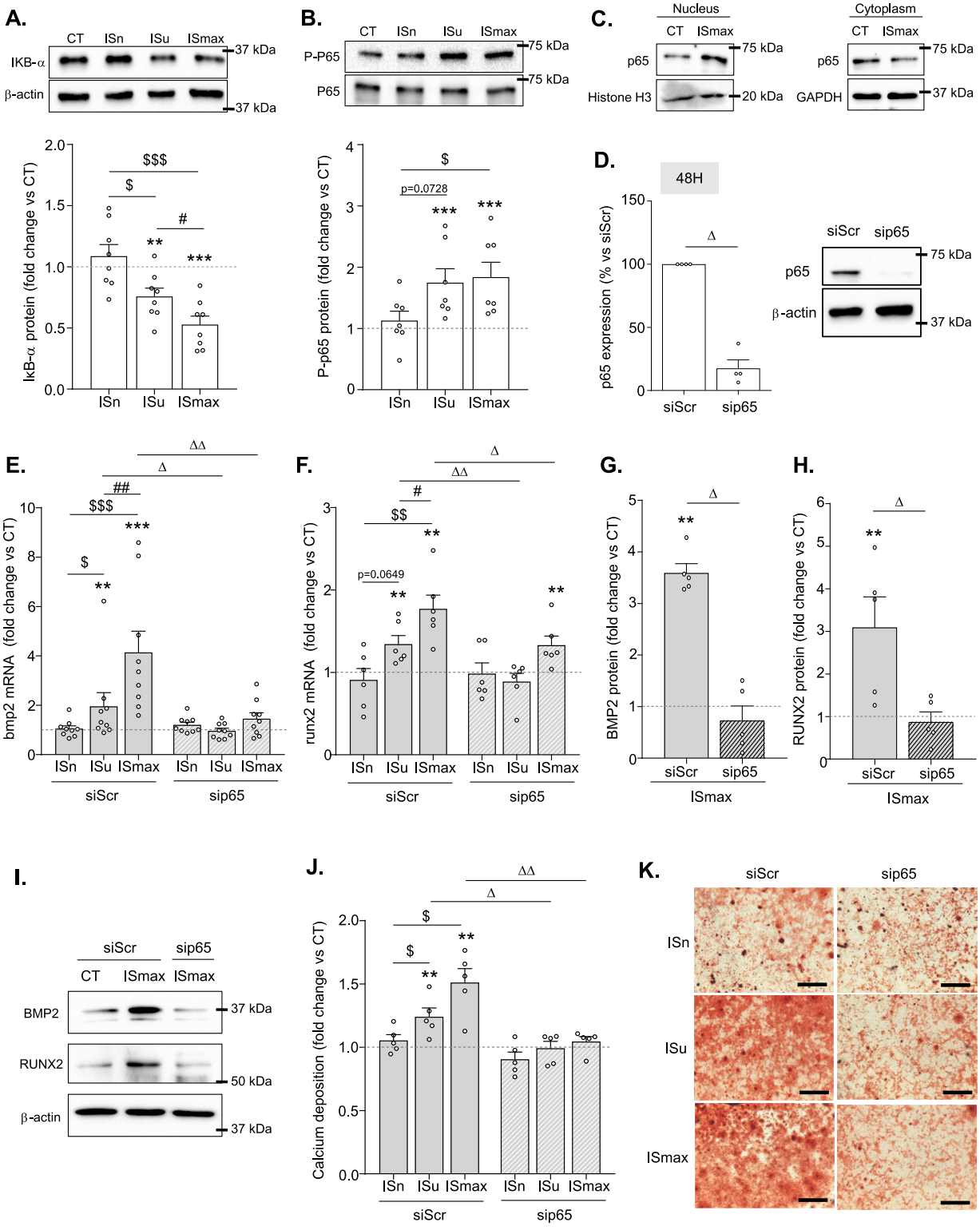

(caption on next page)

Fig. 3. IS-induced activation of the canonical NF-κB pathway promotes hVICs osteogenic transition and calcification. A. and B. Immunoblotting of IKBα (A.) and P-p65 (B.) performed on whole cell lysates prepared from h-VICs stimulated with either ISn, ISu or ISmax for 30 min. Results represent at least six independent experiments. Data are expressed as a fold change vs the control condition (CT: dotted line), which represents cells cultured in the absence of IS. Error bars represent the S.E.M. C. Immunoblotting of p65 performed on the nuclear and cytoplasmic fraction of h-VICs stimulated or not with ISmax for 30 min. Results represent three independent experiments. D. Effects of p65 siRNA on p65 expression in hVICs. Results represent four independent experiments. Error bars represent the S.E.M. E. and F. Impact of a 3-day treatment with ISn, ISu or ISmax on bmp2 (E.) and runx2 (F.) mRNA expression in scrambled (siScr) or p65-siRNA (sip65) transfected hVICs, assessed by qRT-PCR. Results represent at least six independent experiments. Data are expressed as a fold change vs the control condition (CT: dotted line), which represent scramble-transfected cells cultured in the absence of IS. Error bars represent the S.E.M. G.-I. Impact of a 3-day treatment with ISmax on BMP2 (G. and I.) and RUNX2 (H. and I.) protein expression in scrambled (siScr) or p65-siRNA (sip65) transfected hVICs exposed to the OM, assessed by western blot. Results represent five independent experiments. Data are expressed as a fold change vs the control condition (CT: dotted line), which represents scramble-transfected cells cultured in the absence of IS. Error bars represent the S.E.M. J. and K. Impact of ISn, ISu or ISmax on the mineralization of scrambled (siScr) or p65-siRNA (sip65) transfected hVICs. The quantitative determination of calcium concentrations was performed by the O-cresolphtalein complexone method (J.). An alizarin red staining was performed to confirm the data (K.). Results represent five independent experiments. For the quantification of mineral deposition, the mean calcium content per well (measured by the o-cresolphthalein complexone method) was normalized to the mean total protein content. Data are expressed as a fold-change relative to the control condition (CT: dotted line), which represents scramble-transfected cells cultured in the absence of IS. Error bars represent the S.E.M. Scale bars: 500 μm. **p<0.01 and ***p<0.001 vs hVICs exposed to CT. $p<0.05, $$p<0.01 and $$$p<0.001 vs hVICs exposed to ISn. #p<0.05 and ##p<0.01 vs hVICs exposed to ISu. Δp<0.05 and ΔΔp<0.05 sip65 vs siScr.

Under non-calcific conditions, exposure to ISu and ISmax increased the mRNA expression of IL-1β and IL-6 in a concentration-dependent manner (Supplementary Fig. 10.A and B), but failed to further the basal secretion of these cytokines (Supplementary Fig. 10.D and E) as compared to untreated cells. Exposure to ISu and ISmax in OM was associated with relative increases in both the expression and the secretion of IL-1β (Fig. 4.B and E) and IL-6 (Fig. 4.C and F) in a concentration-dependent manner. Exposure to ISu and ISmax under either non-calcific or pro-calcific conditions was associated with greater expression of TNF-α transcripts (relative to ISn-treated cells) in a concentration-dependent manner (Supplementary Fig. 10.C and Fig. 4.D) but failed to induce TNF-α secretion in hVICs (Supplementary Fig. 10.F and Fig. 4.G).

In this hVIC model, the mean ± SEM level of IL-1β produced in response to ISu (0.3 ± 0.1154 pg/mL) or ISmax (0.5878 ± 0.1672 pg/mL) was far below the concentrations described as inducing hVIC calcification in vitro (typically ~10 ng/mL) [20,28]. However, the mean quantity of IL6 secreted in response to ISu (3682 ± 2072 pg/mL) or ISmax (5368 ± 3160 pg/mL) was similar to that known to induce the osteogenic transition of hVICs in vitro [20]. We therefore hypothesized that IL-6 secretion is responsible for IS-induced hVIC osteogenic transition and calcification.

3.6. IS-induced IL-6 secretion promotes the osteogenic transition and calcification of hVICs

To assess IL-6's involvement in IS-induced hVIC osteogenic transition and calcification, cells cultured in OM were then exposed to ISmax in the presence or absence of an antibody against IL-6. Exposure to this antibody significantly attenuated the ISmax-induced elevation in *BMP2* and *RUNX2* expression both at the mRNA (Fig. 5.A and B) and protein (Fig. 5.C-E) level, as compared to vehicle-treated cells. The presence of the antibody during the mineralization assay completely abolished ISmax-induced mineralization of hVICs, relative to vehicle-treated cells (Fig. 5.F and G).

3.7. IS-induced IL-6 expression and secretion depends on the AhR and activation of the NF-κB pathway

Production of IL-6 is a hallmark of NF-κB pathway activation [29]. To determine whether IS-induced IL-6 secretion depended on NF-κB activation, we evaluated the impact of IS on IL-6 expression and secretion in hVICs transfected with siRNA against p65. Downregulation of p65 significantly reduced the elevation of IL-6 transcripts induced by ISu and ISmax under non-calcific conditions (Supplementary Fig. 11.A) and pro-calcific conditions (Fig. 6.A). Downregulation of p65 also reduced the secretion of IL-6 induced by ISu and ISmax in cells cultured in OM (Fig. 6.B).

To determine whether IS-induced IL-6 secretion depended on AhR activation, we evaluated the impact of IS on IL-6 expression and secretion in hVICs transfected with siRNA against the AhR. Downregulation of AhR significantly reduced the elevation of IL-6 transcripts induced by ISu and ISmax under non-calcific conditions (Supplementary Fig. 11.B) and pro-calcific conditions (Fig. 6.C). Downregulation of AhR also lowered the secretion of IL-6 induced by ISu and ISmax in cells cultured in OM (Fig. 6.D).

4. Discussion

Our present results showed that IS promotes the osteogenic transition and calcification of primary hVICs in a direct, concentration-dependent manner. This effect depends on AhR-induced activation of the NF-κB pathway and the subsequent secretion of IL-6, which ultimately promotes the hVICs' osteogenic transition and calcification in an autocrine manner (Fig. 7). To the best of our knowledge, the present study is the first to have shown that IS-induced hVIC inflammation might be a key driver of CKD-related CAS. Given that aortic valve calcification is a well-validated marker of stenosis severity and a powerful predictor of disease progression and adverse events [7,30], our observation that IS promotes the osteogenic transition and calcification of hVICs suggests that elevated IS can worsen outcomes in patients with CKD. Further research should seek to determine whether the degree of CAS is correlated with circulating levels of IS in patients with CKD.

Indoxyl sulfate is an endogenous ligand of the transcription factor AhR; as mentioned above, it is now well established that AhR mediates most of the harmful cardiovascular effects of IS [15–17]. To the best of our knowledge, the present study is the first to have demonstrated that hVICs express a functional AhR. In patients with cardiovascular disease, AhR activation mediates vascular inflammation, changes in the phenotype of vascular cells, vascular remodeling, and atherogenesis [17,31]. AhR signaling is also associated with many age-related degenerative processes [32]. Here, we found that AhR has a pivotal role in IS-induced hVIC osteogenic differentiation and mineralization by promoting the NF-κB-mediated activation of IL-6 secretion. Future studies should evaluate whether the antagonism of AhR with compounds such as resveratrol (which efficiently prevents the osteogenic transition and calcification of cardiovascular cells [33–35]) slows down hVIC mineralization in a CKD setting.

Our results further showed that IS-induced IL-6 secretion in hVICs depends on activation of the NF-κB pathway, the blockade of which reduced IL-6 secretion and subsequent osteogenic differentiation and calcification. These observations are in line with previous reports in which the IS-induced calcification of aortic VSMCs depended on NF-κB activation [36]. Furthermore, the induction of the NF-κB signaling pathway has a critical role in the development and progression of CAS [37,38]. Indeed, the NF-κB-induced expression of *BMP2* and *RUNX2* promotes hVIC mineralization [26,37,38]. In this context, it is

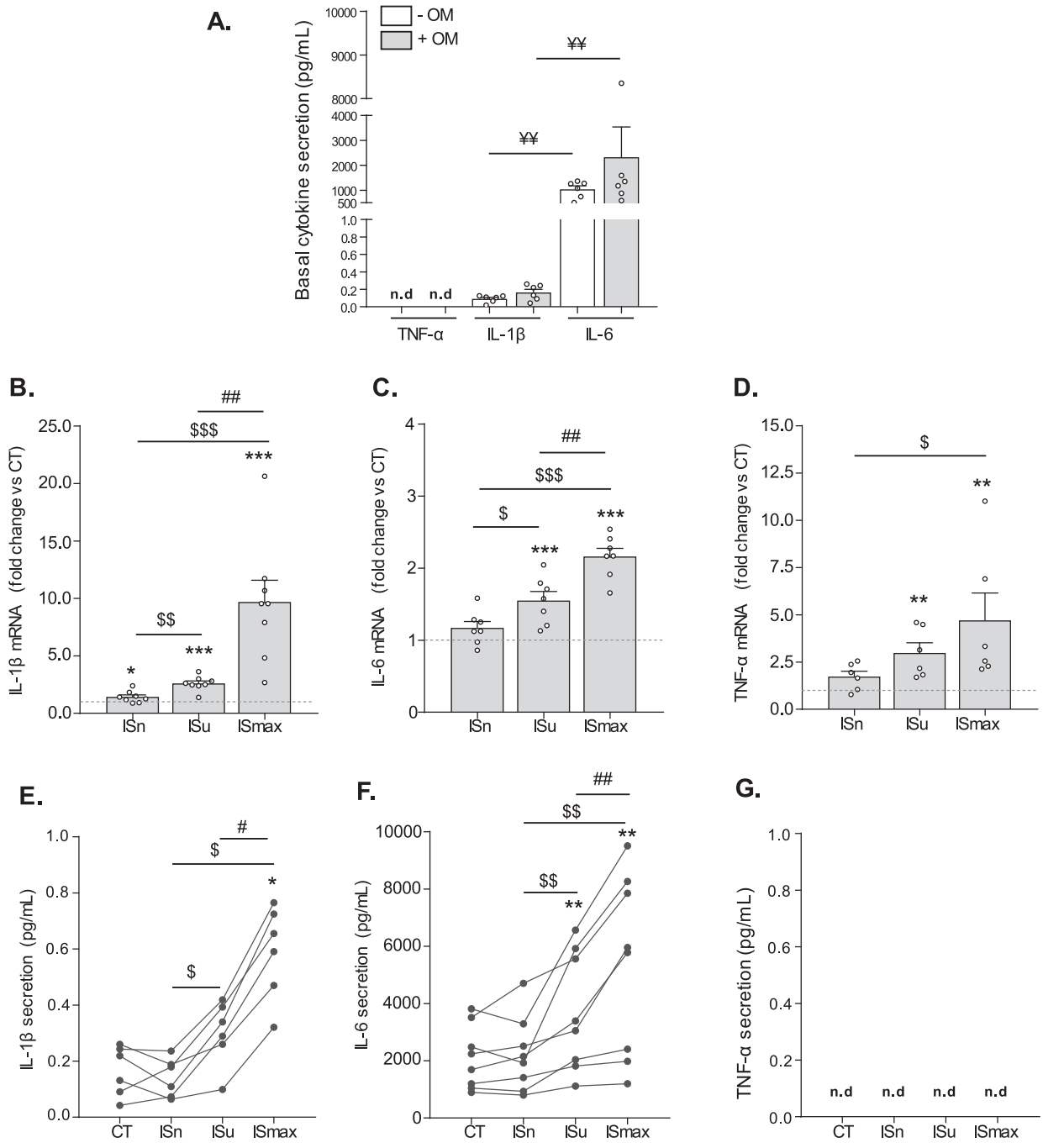

Fig. 4. IS promotes hVICs secretion of both IL-6 and IL-1β but not TNF-α. A. Evaluation by ELISA of TNF-α, IL-1β and IL-6 basal secretion by primary hVICs exposed for 3 days to the non-calcific or the pro-calcific medium. Results represent six independent experiments. Error bars represent the S.E.M. ¥p<0.05 and ¥¥p<0.01: IL-6 secretion vs IL-1β secretion. B—D. Impact of a 3-day treatment with ISn, ISu or ISmax on IL-1β (B.), IL-6 (C.) and TNF-α (D.) mRNA expression, assessed by qRT-PCR. Results represent at least six independent experiments. Data are expressed as a fold change vs the control condition (CT: dotted line), which represents cells cultured in the absence of IS. Error bars represent the S.E.M. E–G. Impact of a 3-day treatment with ISn, ISu or ISmax on IL-1β (E.), IL-6 (F.) and TNF-α (G.) secretion, assessed by ELISA. Results represent at least six independent experiments. Data are expressed as a fold change vs the control condition (CT: dotted line), which represents cells cultured in the absence of IS. *p<0.05, **p<0.01 and ***p<0.001 vs hVICs exposed to CT. $p<0.05, $$p<0.01 and $$$p<0.001vs hVICs exposed to ISn. #p<0.05 and ##p<0.01 vs hVICs exposed to ISu. OM: osteogenic medium.

noteworthy that reducing the level of NF-κB-induced autocrine inflammation in hVICs (using the JAK inhibitor ruxolitinib) prevents the osteogenic transition and calcification [39]. Similar data were obtained following the inhibition of NF-κB-induced RUNX2 activation with hydrogen sulfide [38]. Therefore, in the current absence of effective ways of reducing IS levels, future research should seek to determine whether the use of agents such as ruxolitinib or hydrogen sulfide can prevent IS's pro-calcific effects on hVICs.

Expression of IL-6 is elevated in aortic valve leaflets isolated from patients with CAS, and this elevation is correlated with the remodeling process [40]. In vitro, primary cultures of human VICs isolated from CAS patients express high levels of IL-6 [40]. We found here that hVICs from CAS patients secrete three times more IL-6 than unpolarized THP1-derived macrophages in basal culture conditions (hVICs: 1037 ±

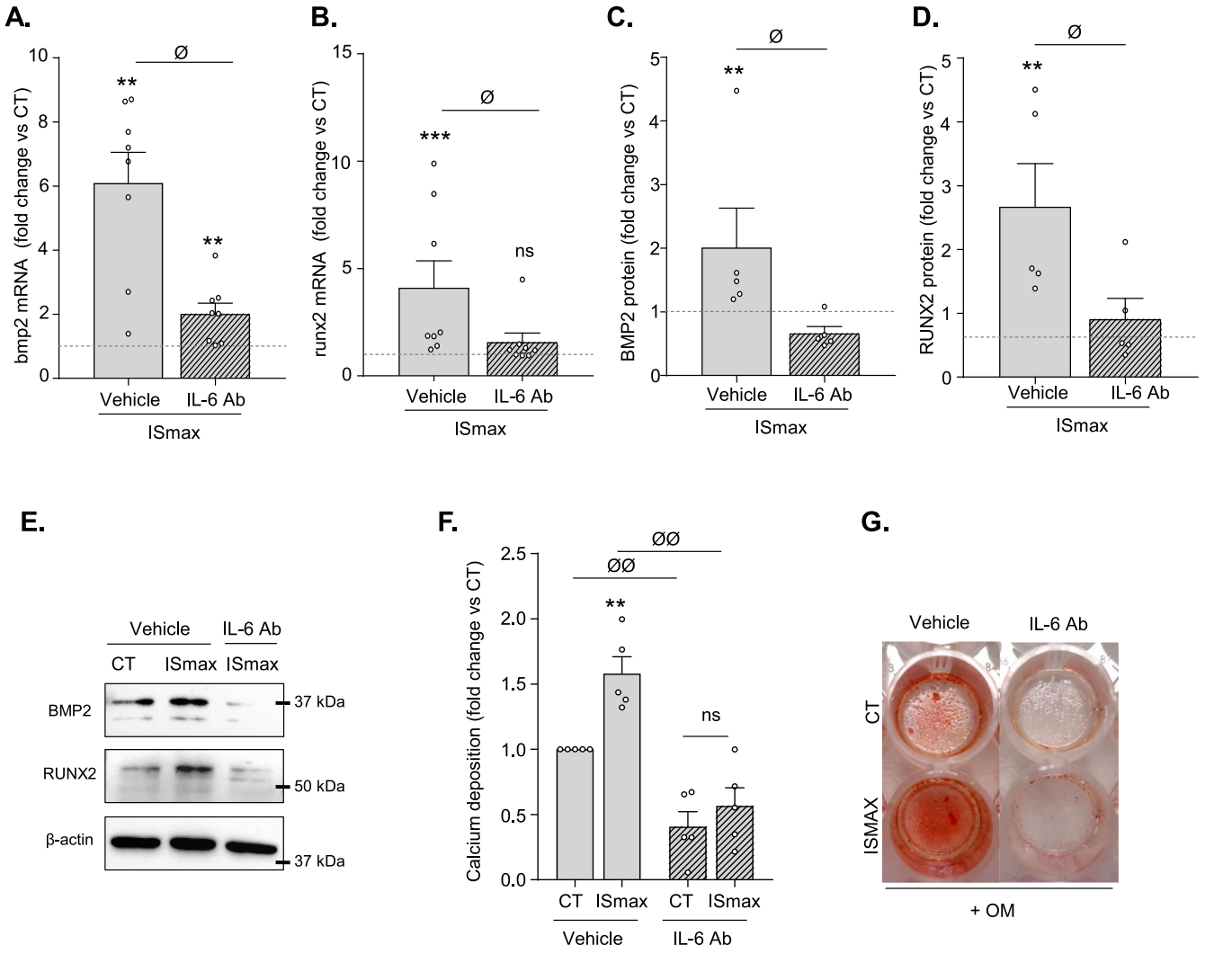

Fig. 5. IS-induced IL-6 secretion promotes hVICs osteogenic transition and calcification. A. and B. Impact of IS on bmp2 (A.) and runx2 (B.) mRNA expression in hVICs cultured in the OM in the presence or absence of an antibody-neutralizing IL-6 (IL-6 Ab). The expression of bmp2 and runx2 transcripts was assessed by qRT-PCR following 3 days of treatment. Results represent eight independent experiments. Data are expressed as a fold change vs the control condition (CT: dotted line), which represents vehicle-treated cells cultured in the absence of IS. Error bars represent the S.E.M. C.-E. Impact of IS on BMP2 (C. and E) and RUNX2 (D. and E) protein expression in hVICs cultured in the OM in the presence or absence of an antibody-neutralizing IL-6 (IL-6 Ab). The impact of IS on BMP2 and RUNX2 expression was assessed by western blot following 3 days of treatment. Results represent five independent experiments. Data are expressed as a fold change vs the control condition (CT: dotted line), which represents vehicle-treated cells cultured in the absence of IS. Error bars represent the S.E.M. F. and G. Impact of IS on the mineralization of hVICs cultured in the OM in the presence or absence of an antibody-neutralizing IL-6 (IL-6 Ab). The quantitative determination of calcium concentrations was performed by the O-cresolphtalein complexone method (F.). An alizarin red staining was performed to confirm the data (G.). Results represent five independent experiments. For the quantification of mineral deposition, the mean calcium content per well (measured by the o-cresolphthalein complexone method) was normalized to the mean total protein content. Data are expressed as a fold-change relative to the control condition (CT: dotted line), which represents vehicle-treated cells cultured in the absence of IS. **p<0.01 and ***p<0.001 vs hVICs exposed to CT. Øp<0.05 and ØØp<0.01: IL-6 Ab vs vehicle.

343.5 pg/mL; macrophages: 344.9 ± 65.79 pg/mL, p=0.012) (Supplementary Fig. 12.A). We also found that the hVICs' basal secretion of IL-6 is amplified by IS and that the mean quantity of IL-6 produced in response to ISu (3682 ± 2072 pg/mL) and ISmax (5368 ± 3160 pg/mL) is similar to that known to induce the osteogenic transition of hVICs in vitro [20]. These findings indicate that under certain pathological conditions (e.g. CKD), hVICs can secrete more IL-6 than immune cells do – thereby promoting their osteogenic transition and calcification in an autocrine manner. Our present findings support Adelibieke et al.'s report in which IS strongly induced the production of IL-6 in both vascular endothelial cells and vascular smooth muscle cells [16]; this might explain why treatment with the oral sorbent AST-120 is associated with a reduction in serum IL-6 levels in patients on dialysis [41].

In 2014, El Husseini et al. reported that a treatment of hVICs with a phosphate-containing medium can double the cells' production of IL-6 [40]. In our model, exposure to OM in the absence of IS did not promote IL-6 secretion. However, neutralization of IL-6 completely blocked OM-induced calcification and thus confirmed El Husseini et al.'s observation of IL-6-dependent, phosphate-induced hVIC mineralization.

We found that exposure of hVICs to ISu and ISmax in OM was also associated with greater, concentration-dependent secretion of IL-1β. However, the mean quantity of IL-1β produced in response to ISu or ISmax was far below that described as inducing hVIC modifications in vitro [20,28]. Our observation is in line with a report showing that IS promotes the production of Il-1β by THP1-derived macrophages by activating AhR/NF-κB cascades but not the NLRP3 inflammasome; mature IL-1 levels were only slightly elevated in these cells [42]. Taken as a whole, these data suggest that IL-1β secretion by hVICs (which was

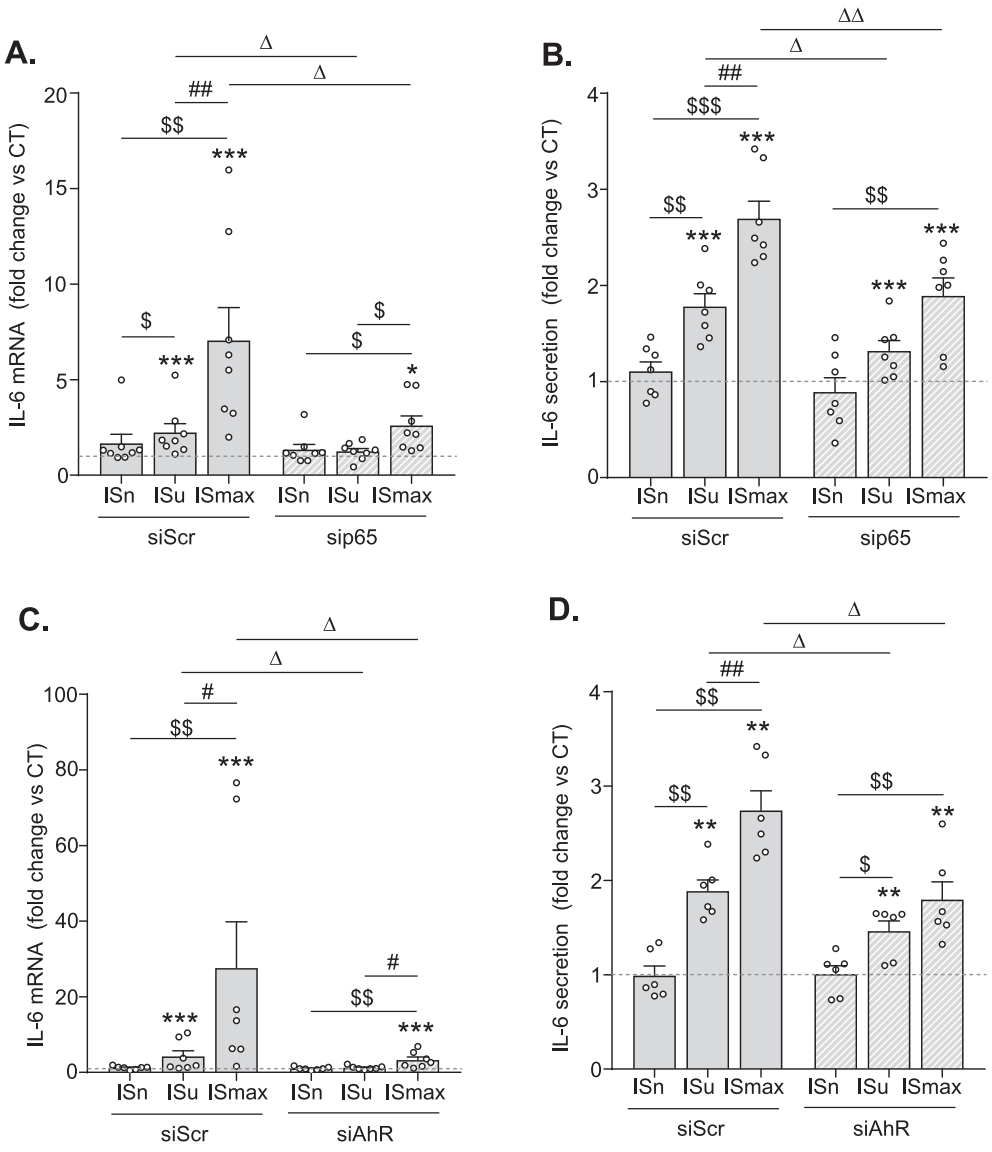

Fig. 6. IS-induced IL-6 expression and secretion depends on AhR and NF-κB pathway activation. A. Impact of IS on IL-6 mRNA expression in scrambled (siScr) or p65-siRNA (sip65) transfected hVICs cultured in the OM. Analysis of IL-6 transcripts was monitored by qRT-PCR, following 3 days of treatment. Results represent eight independent experiments. Data are expressed as a fold change vs the control condition (CT: dotted line), which represents cells cultured in the absence of IS. Error bars represent the S.E.M. B. Impact of IS on IL-6 secretion in scrambled (siScr) or p65-siRNA (sip65) transfected hVICs cultured in the OM. Analysis of IL-6 secretion was monitored by ELISA following 3 days of treatment. Results represent seven independent experiments. Data are expressed as a fold change vs the control condition (CT: dotted line), which represents cells cultured in the absence of IS. Error bars represent the S.E.M.
C. Impact of IS on IL-6 expression in scrambled (siScr) or AhR-siRNA (siAhR) transfected hVICs cultured in the OM. Analysis of IL-6 transcripts was monitored by qRT-PCR, following 3 days of treatment. Results represent seven independent experiments. Data are expressed as a fold change vs the control condition (CT: dotted line), which represents cells cultured in the absence of IS. Error bars represent the S.E.M. D. Impact of IS on IL-6 secretion in scrambled (siScr) or AhR-siRNA (siAhR) transfected hVICs cultured in the OM. Analysis of IL-6 secretion was monitored by ELISA following 3 days of treatment. Results represent six independent experiments. Data are expressed as a fold change vs the control condition (CT: dotted line), which represents cells cultured in the absence of IS. Error bars represent the S.E.M.
**p<0.01 and ***p<0.001 vs hVICs exposed to CT. $p<0.05, $$p<0.01 and $$$p<0.001 vs hVICs exposed to ISn. #p<0.05 and ##p<0.01 vs hVICs exposed to ISu. Δp<0.05 and ΔΔp<0.01 vs scrambled-transfected hVICs.

around 4000-fold lower in hVICs (0.0915 ± 0.042 pg/mL) than in macrophages (414.4 ± 191.23 pg/mL; p=0.012; supplementary Fig. 12. B) is unlikely to be involved in IS's pro-calcific effects. In our model, hVICs were unable to secrete TNF-α even when cultured in an OM supplemented with IS. This finding is in line with a report whereby hVICs do not secrete TNF-α in response to LPS [43] and suggests that local production of TNF-α by hVICs is unlikely to be involved in the progression of CAS. The key role of IL-6 in IS-induced hVIC mineralization highlighted in our model is also supported by the finding that IL-1β and TNF-α do not promote *RUNX2* activation in hVICs [20].

A growing body of evidence indicates that IL-6 has a key role in CKD-related cardiovascular calcification [44]. Indeed, IL-6 is one of the inflammation biomarkers that best predicts the clinical outcome in patients with CKD [45]. Interestingly, Vidula et al.'s study of a large cohort of 940 patients with AS and a normal renal function showed that circulating levels of IL-6 are strongly associated with the risk of adverse outcomes [46]. To date, the relationship between circulating levels of IL-6 and the severity of CAS in patients with CKD has not been investigated. The fact that IL-6 neutralization blocks IS pro-calcific effects in our model is therefore of particular interest because ziltivekimab (a monoclonal antibody against IL-6) is currently in clinical investigation in patients with stage 3–5 CKD [47,48]. When administered to dialyzed patients who respond poorly to erythropoiesis-stimulating agents, ziltivekimab was well tolerated and was associated with a reduction in inflammation marker levels and anemia and better nutritional status [49]. The ongoing Ziltivekimab Cardiovascular Outcomes Study, which objective is to compare ziltivekimab with placebo in 6200 patients with stage 3–4 CKD and elevated serum levels of high-sensitivity C-reactive protein, should soon provide formal evidence of whether or not reducing circulating IL-6 levels leads to a decrease in the cardiovascular event rate [50]. If the clinical outcomes are positive, further studies will have to determine whether treatment with ziltivekimab also slows the progression of CAS in a CKD setting.

5. Conclusion

Activation of the AhR- NF-κB pathway by IS promoted the osteogenic transition and calcification of primary hVICs. We found that the

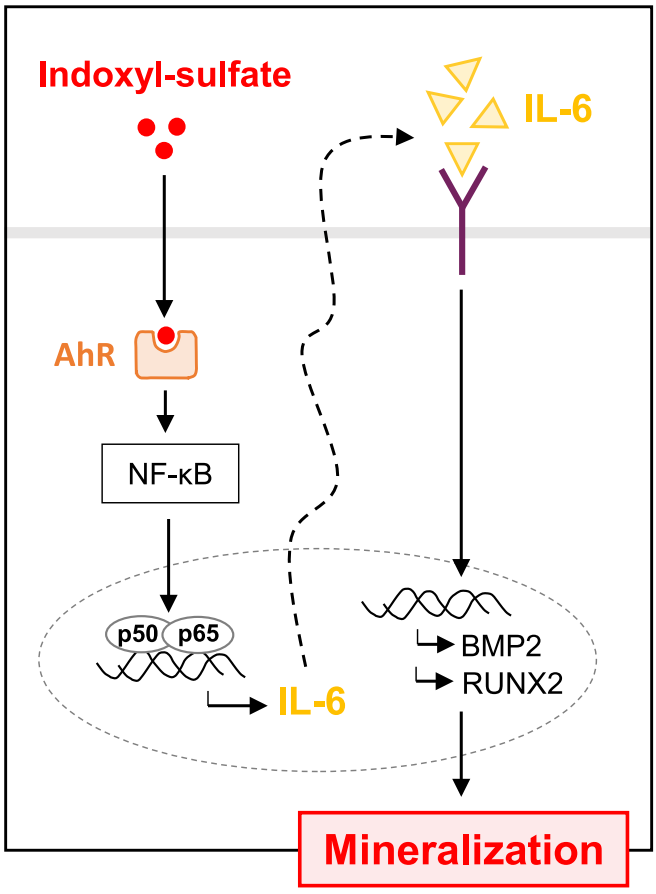

Fig. 7. Indoxyl-sulfate activation of the AhR- NF-κB pathway promotes IL-6 secretion and subsequent osteogenic differentiation and mineralization of human valvular interstitial cells from the aortic valve: A schematic view.

secretion of IL-6 following activation of the AhR- NF-κB pathway is a crucial event in the osteogenic transition and subsequent calcification of hVICs. We showed that molecular interventions that block NF-κB pathway activation or IL-6 secretion efficaciously reduced the IS-induced osteogenic transition and calcification of hVICs in vitro. Since the conclusions drawn in this manuscript are exclusively based on in vitro data, further studies will be needed to confirm the role played by IS on the development of AS and subsequent cardiac dysfunction in animal models of CKD. In the absence of effective ways of reducing IS levels, future research should seek to determine whether targeting inflammatory pathways in this animal model can reduce the onset and progression of CKD-related CAS. Lastly, our findings suggest that the impact of alternative IS-lowering strategies (such as the use of oral sorbents like AST-120, the modulation of gut microbiota with probiotics, or the preservation of residual kidney function via peritoneal dialysis) should also be investigated in the context of CKD-related aortic stenosis.

Funding

This work was supported by the French government's *Investissements d'Avenir* program (reference: ANR-16-RHUS-0003_STOP-AS, managed by the French National Research Agency), the *Fédération Hospitalo-Universitaire* program "CArdiac Research Network on Aortic VAlve and heart failure" (reference: GCS G4 FHU CARNAVAL), the Fédération Hospitalo-Universitaire program "Early Markers of Cardiovascular Remodeling in Valvulopathy and Heart Failure" (reference: GCS G4 FHU REMOD VHF) and the Hauts-de-France Regional Council.

Authors' contributions

LH, SK, AC, CB, MB and GC conceived the study. CT, TC and CA collected human aortic valve samples and isolated hVICs from non-calcified areas of the valves. NI, AC, GB and LH cultured hVICs and performed mineralization assays. NI and LH performed transfections. NI, AC, MG, TB and CB performed mRNA extraction and PCR analyses. CB and NI performed protein extractions and western blots. NI and AC performed MTT and TUNEL assays. CG and BG performed ELISA experiments. LH, AC, CB, NI and YB performed data analysis and interpretation. LH and AC designed the figs. AC, LH and CB wrote the paper. SK, GC, YB, MB and CT critically reviewed the study and the manuscript.

Declaration of Competing Interest

None.

Data availability statement

The data that support the findings of this study are available from the corresponding author upon request.

Acknowledgements

The authors thank Lucie Moussot for technical assistance with ELISA experiments.

Appendix A. Supplementary data

Supplementary data to this article can be found online at https://doi.org/10.1016/j.yjmcc.2023.03.011.

References

[1] G. Vavilis, M. Bäck, G. Occhino, et al., Kidney dysfunction and the risk of developing aortic stenosis, J. Am. Coll. Cardiol. 73 (2019) 305–314, https://doi.org/10.1016/j.jacc.2018.10.068.
[2] D. Zentner, D. Hunt, W. Chan, F. Barzi, L. Grigg, V. Perkovic, Prospective evaluation of aortic stenosis in end-stage kidney disease: a more fulminant process? Nephrol. Dial. Transplant. 26 (2011) 1651–1655, https://doi.org/10.1093/ndt/gfq596.
[3] P. Ureña-Torres, L. D'Marco, P. Raggi, et al., Valvular heart disease and calcification in CKD: more common than appreciated, Nephrol. Dial. Transplant. 35 (2020) 2046–2053, https://doi.org/10.1093/ndt/gfz133.
[4] G.R. Shroff, S. Bangalore, N.M. Bhave, et al., Evaluation and Management of Aortic Stenosis in Chronic Kidney Disease: A Scientific Statement from the American Heart Association, Circulation 143 (2021) e1088–e1114, https://doi.org/10.1161/CIR.0000000000000979.
[5] Y. Bohbot, A. Candellier, M. Diouf, et al., Severe aortic stenosis and chronic kidney disease: outcomes and impact of aortic valve replacement, J. Am. Heart Assoc. 9 (2020), e017190, https://doi.org/10.1161/JAHA.120.017190.
[6] M. Szerlip, A. Zajarias, S. Vemalapalli, et al., Transcatheter aortic valve replacement in patients with end-stage renal disease, J. Am. Coll. Cardiol. 73 (2019) 2806–2815, https://doi.org/10.1016/j.jacc.2019.03.496.
[7] T. Pawade, T. Sheth, E. Guzzetti, M.R. Dweck, M.A. Clavel, Why and how to measure aortic valve calcification in patients with aortic stenosis, JACC Cardiovasc. Imaging 12 (2019) 1835–1848, https://doi.org/10.1016/j.jcmg.2019.01.045.
[8] A.C. Liu, V.R. Joag, A.I. Gotlieb, The emerging role of valve interstitial cell phenotypes in regulating heart valve pathobiology, Am. J. Pathol. 171 (2007) 1407–1418, https://doi.org/10.2353/ajpath.2007.070251.
[9] K.I. Boström, N.M. Rajamannan, D.A. Towler, The regulation of valvular and vascular sclerosis by osteogenic morphogens, Circ. Res. 109 (2011) 564–577, https://doi.org/10.1161/CIRCRESAHA.110.234278.
[10] T.H. Marwick, K. Amann, S. Bangalore, et al., Chronic kidney disease and valvular heart disease: conclusions from a kidney disease: improving global Outcomes (KDIGO) Controversies Conference, Kidney Int. 96 (2019) 836–849, https://doi.org/10.1016/j.kint.2019.06.025.
[11] F.C. Barreto, D.V. Barreto, S. Liabeuf, et al., Serum indoxyl sulfate is associated with vascular disease and mortality in chronic kidney disease patients, Clin. J. Am. Soc. Nephrol. 4 (2009) 1551–1558, https://doi.org/10.2215/CJN.03980609.
[12] G. Muteliefu, A. Enomoto, P. Jiang, M. Takahashi, T. Niwa, Indoxyl sulphate induces oxidative stress and the expression of osteoblast-specific proteins in vascular smooth muscle cells, Nephrol. Dial. Transplant. 24 (2009) 2051–2058, https://doi.org/10.1093/ndt/gfn757.

[13] G. Muteliefu, H. Shimizu, A. Enomoto, F. Nishijima, M. Takahashi, T. Niwa, Indoxyl sulfate promotes vascular smooth muscle cell senescence with upregulation of p53, p21, and prelamin A through oxidative stress, Am. J. Phys. Cell Phys. 303 (2012) C126–C134, https://doi.org/10.1152/ajpcell.00329.2011.
[14] A. Adijiang, S. Goto, S. Uramoto, F. Nishijima, T. Niwa, Indoxyl sulphate promotes aortic calcification with expression of osteoblast-specific proteins in hypertensive rats, Nephrol. Dial. Transplant. 23 (2008) 1892–1901, https://doi.org/10.1093/ndt/gfm861.
[15] C. Nguyen, A.J. Edgley, D.J. Kelly, A.R. Kompa, Aryl hydrocarbon receptor inhibition restores indoxyl sulfate-mediated endothelial dysfunction in rat aortic rings, Toxins (Basel) 14 (2022) 100, https://doi.org/10.3390/toxins14020100.
[16] Y. Adelibieke, M. Yisireyili, H.Y. Ng, S. Saito, F. Nishijima, T. Niwa, Indoxyl sulfate induces IL-6 expression in vascular endothelial and smooth muscle cells through OAT3-mediated uptake and activation of AhR/NF-κB pathway, Nephron Exp. Nephrol. 128 (2014) 1–8, https://doi.org/10.1159/000365217.
[17] M. Sallée, L. Dou, C. Cerini, S. Poitevin, P. Brunet, S. Burtey, The aryl hydrocarbon receptor-activating effect of uremic toxins from tryptophan metabolism: a new concept to understand cardiovascular complications of chronic kidney disease, Toxins (Basel) 6 (2014) 934–949, https://doi.org/10.3390/toxins6030934.
[18] N. Latif, A. Quillon, P. Sarathchandra, et al., Modulation of human valve interstitial cell phenotype and function using a fibroblast growth factor 2 formulation, PLoS One 10 (2015), e0127844, https://doi.org/10.1371/journal.pone.0127844.
[19] E. Nagy, P. Eriksson, M. Yousry, et al., Valvular osteoclasts in calcification and aortic valve stenosis severity, Int. J. Cardiol. 168 (2013) 2264–2271, https://doi.org/10.1016/j.ijcard.2013.01.207.
[20] J.C. Grim, B.A. Aguado, B.J. Vogt, et al., Secreted factors from proinflammatory macrophages promote an osteoblast-like phenotype in valvular interstitial cells, Arterioscler. Thromb. Vasc. Biol. 40 (2020) e296–e308, https://doi.org/10.1161/ATVBAHA.120.315261.
[21] J. Hao, J. Tang, L. Zhang, X. Li, L. Hao, The crosstalk between calcium ions and aldosterone contributes to inflammation, apoptosis, and calcification of VSMC via the AIF-1/NF, Oxidative Med. Cell. Longev. 2020 (2020) 3431597, https://doi.org/10.1155/2020/3431597.
[22] J. Voelkl, T.T. Luong, R. Tuffaha, et al., SGK1 induces vascular smooth muscle cell calcification through NF-κB signaling, J. Clin. Invest. 128 (2018) 3024–3040, https://doi.org/10.1172/JCI96477.
[23] H.Y. Kim, T.H. Yoo, J.Y. Cho, H.C. Kim, W.W. Lee, Indoxyl sulfate-induced TNF-α is regulated by crosstalk between the aryl hydrocarbon receptor, NF-κB, and SOCS2 in human macrophages, FASEB J. 33 (2019) 10844–10858, https://doi.org/10.1096/fj.201900730R.
[24] P.H. Chen, H. Chang, J.T. Chang, P. Lin, Aryl hydrocarbon receptor in association with RelA modulates IL-6 expression in non-smoking lung cancer, Oncogene 31 (2012) 2555–2565, https://doi.org/10.1038/onc.2011.438.
[25] M. Karin, M. Delhase, The I kappa B kinase (IKK) and NF-kappa B: key elements of proinflammatory signalling, Semin. Immunol. 12 (2000) 85–98, https://doi.org/10.1006/smim.2000.0210.
[26] Z. Yu, K. Seya, K. Daitoku, S. Motomura, I. Fukuda, K. Furukawa, Tumor necrosis factor-α accelerates the calcification of human aortic valve interstitial cells obtained from patients with calcific aortic valve stenosis via the BMP2-Dlx5 pathway, J. Pharmacol. Exp. Ther. 337 (2011) 16–23, https://doi.org/10.1124/jpet.110.177915.
[27] K. Matsuo, S. Yamamoto, T. Wakamatsu, et al., Increased proinflammatory cytokine production and decreased cholesterol efflux due to downregulation of abcg1 in macrophages exposed to indoxyl sulfate, Toxins (Basel) 7 (2015) 3155–3166, https://doi.org/10.3390/toxins7083155.
[28] J.J. Kaden, C.E. Dempfle, R. Grobholz, et al., Interleukin-1 beta promotes matrix metalloproteinase expression and cell proliferation in calcific aortic valve stenosis, Atherosclerosis 170 (2003) 205–211, https://doi.org/10.1016/s0021-9150(03)00284-3.
[29] A.R. Brasier, The nuclear factor-kappaB-interleukin-6 signalling pathway mediating vascular inflammation, Cardiovasc. Res. 86 (2010) 211–218, https://doi.org/10.1093/cvr/cvq076.
[30] R. Rosenhek, T. Binder, G. Porenta, et al., Predictors of outcome in severe, asymptomatic aortic stenosis, N. Engl. J. Med. 343 (2000) 611–617, https://doi.org/10.1056/NEJM200008313430903.
[31] L. Pernomian, C.H.T.P. da Silva, Current basis for discovery and development of aryl hydrocarbon receptor antagonists for experimental and therapeutic use in atherosclerosis, Eur. J. Pharmacol. 764 (2015) 118–123, https://doi.org/10.1016/j.ejphar.2015.06.058.
[32] A. Salminen, Aryl hydrocarbon receptor (AhR) reveals evidence of antagonistic pleiotropy in the regulation of the aging process, Cell. Mol. Life Sci. 79 (2022) 489, https://doi.org/10.1007/s00018-022-04520-x.
[33] X. Huang, Y. Wang, Y. Qiu, et al., Resveratrol ameliorates high-phosphate-induced VSMCs to osteoblast-like cells transdifferentiation and arterial medial calcification in CKD through regulating Wnt/β-catenin signaling, Eur. J. Pharmacol. 925 (2022), 174953, https://doi.org/10.1016/j.ejphar.2022.174953.
[34] S.K. Hammad, R.G. Eissa, M.A. Shaheen, N.N. Younis, Resveratrol ameliorates aortic calcification in ovariectomized rats via SIRT1 signaling, Curr. Iss. Mol. Biol. 43 (2021) 1057–1071, https://doi.org/10.3390/cimb43020075.
[35] J. Lee, S.W. Hong, M.J. Kim, et al., Metformin, resveratrol, and exendin-4 inhibit high phosphate-induced vascular calcification via AMPK-RANKL signaling, Biochem. Biophys. Res. Commun. 530 (2020) 374–380, https://doi.org/10.1016/j.bbrc.2020.07.136.
[36] X. He, H. Jiang, F. Gao, S. Liang, M. Wei, L. Chen, Indoxyl sulfate-induced calcification of vascular smooth muscle cells via the PI3K/Akt/NF-κB signaling pathway, Microsc. Res. Tech. 82 (2019) 2000–2006, https://doi.org/10.1002/jemt.23369.
[37] D. Wang, Q. Zeng, R. Song, L. Ao, D.A. Fullerton, X. Meng, Ligation of ICAM-1 on human aortic valve interstitial cells induces the osteogenic response: a critical role of the Notch1-NF-κB pathway in BMP-2 expression, Biochim. Biophys. Acta 1843 (2014) 2744–2753, https://doi.org/10.1016/j.bbamcr.2014.07.017.
[38] K. Éva Sikura, Z. Combi, L. Potor, et al., Hydrogen sulfide inhibits aortic valve calcification in heart via regulating RUNX2 by NF-κB, a link between inflammation and mineralization, J. Adv. Res. 27 (2021) 165–176, https://doi.org/10.1016/j.jare.2020.07.005.
[39] I. Parra-Izquierdo, T. Sánchez-Bayuela, I. Castaños-Mollor, et al., Clinically used JAK inhibitor blunts dsRNA-induced inflammation and calcification in aortic valve interstitial cells, FEBS J. 288 (2021) 6528–6542, https://doi.org/10.1111/febs.16026.
[40] D. El Husseini, M.C. Boulanger, A. Mahmut, et al., P2Y2 receptor represses IL-6 expression by valve interstitial cells through Akt: implication for calcific aortic valve disease, J. Mol. Cell. Cardiol. 72 (2014) 146–156, https://doi.org/10.1016/j.yjmcc.2014.02.014.
[41] C.T. Lee, C.Y. Hsu, Y.L. Tain, et al., Effects of AST-120 on blood concentrations of protein-bound uremic toxins and biomarkers of cardiovascular risk in chronic dialysis patients, Blood Purif. 37 (2014) 76–83, https://doi.org/10.1159/000357641.
[42] T. Wakamatsu, S. Yamamoto, T. Ito, et al., Indoxyl sulfate promotes macrophage IL-1β production by activating aryl hydrocarbon receptor/NF-κ/MAPK cascades, but the NLRP3 inflammasome was not activated, Toxins (Basel) 10 (2018) 124, https://doi.org/10.3390/toxins10030124.
[43] G. Karadimou, O. Plunde, S.C. Pawelzik, et al., TLR7 expression is associated with M2 macrophage subset in calcific aortic valve stenosis, Cells 9 (2020) 1710, https://doi.org/10.3390/cells9071710.
[44] L. Hénaut, Z.A. Massy, New insights into the key role of interleukin 6 in vascular calcification of chronic kidney disease, Nephrol. Dial. Transplant. 33 (2018) 543–548, https://doi.org/10.1093/ndt/gfx379.
[45] D.V. Barreto, F.C. Barreto, S. Liabeuf, et al., Plasma interleukin-6 is independently associated with mortality in both hemodialysis and pre-dialysis patients with chronic kidney disease, Kidney Int. 77 (2010) 550–556, https://doi.org/10.1038/ki.2009.503.
[46] M.K. Vidula, A. Orlenko, L. Zhao, et al., Plasma biomarkers associated with adverse outcomes in patients with calcific aortic stenosis, Eur. J. Heart Fail. 23 (2021) 2021–2032, https://doi.org/10.1002/ejhf.2361.
[47] P.M. Ridker, M. Devalaraja, F.M.M. Baeres, et al., IL-6 inhibition with ziltivekimab in patients at high atherosclerotic risk (RESCUE): a double-blind, randomised, placebo-controlled, phase 2 trial, Lancet 397 (2021) 2060–2069, https://doi.org/10.1016/S0140-6736(21)00520-1.
[48] P.M. Ridker, From RESCUE to ZEUS: will interleukin-6 inhibition with ziltivekimab prove effective for cardiovascular event reduction? Cardiovasc. Res. 117 (Sep 2021) e138–e140, https://doi.org/10.1093/cvr/cvab231.
[49] P.E. Pergola, M. Devalaraja, S. Fishbane, et al., Ziltivekimab for treatment of Anemia of Inflammation in Patients on Hemodialysis: results from a Phase 1/2 multicenter, randomized, double-blind, Placebo-Controlled Trial, J. Am. Soc. Nephrol. 32 (2021) 211–222, https://doi.org/10.1681/ASN.2020050595.
[50] P.M. Ridker, M. Rane, Interleukin-6 signaling and anti-interleukin-6 therapeutics in cardiovascular disease, Circ. Res. 128 (2021) 1728–1746, https://doi.org/10.1161/CIRCRESAHA.121.319077.

Glossary

AhR: aryl hydrocarbon receptor
AVR: aortic valve replacement
Bmp2: bone morphogenetic protein 2
CAS: calcific aortic stenosis
CKD: chronic kidney disease
HVICs: human valvular interstitial cells
IκBα: NF kappa B inhibitor α
IL-6: interleukin 6
IL-1β: interleukin 1β
IS: indoxyl-sulfate
ISn: normal concentration of indoxyl-sulfate
ISu: average uremic concentration of indoxyl-sulfate
ISmax: maximum uremic concentration of indoxyl-sulfate
NF-κB: nuclear factor-kappa B
OM: osteogenic medium
Runx2: runt-related transcription factor 2
siRNA: small interfering RNA
siAhR: siRNA targeting AhR
sip65: siRNA targeting p65
siScr: scrambled siRNA
TNF-α: tumor necrosis factor α